New procedure of quantitative mapping of Ti and Al released from dental implant and Mg, Ca, Fe, Zn, Cu, Mn as physiological elements in oral mucosa by LA-ICP-MS

Article *in* Talanta · July 2017

DOI: 10.1016/j.talanta.2017.07.058

CITATIONS
3

READS
123

4 authors, including:

Adam Sajnóg
Adam Mickiewicz University
12 PUBLICATIONS **148** CITATIONS
SEE PROFILE

Anetta Hanć
Adam Mickiewicz University
41 PUBLICATIONS **301** CITATIONS
SEE PROFILE

Ryszard Koczorowski
Poznan University of Medical Sciences
63 PUBLICATIONS **223** CITATIONS
SEE PROFILE

Talanta 175 (2017) 370–381

Contents lists available at ScienceDirect

Talanta

journal homepage: www.elsevier.com/locate/talanta

New procedure of quantitative mapping of Ti and Al released from dental implant and Mg, Ca, Fe, Zn, Cu, Mn as physiological elements in oral mucosa by LA-ICP-MS

Adam Sajnóg[a], Anetta Hanć[a], Ryszard Koczorowski[b], Danuta Barałkiewicz[a,*]

[a] Department of Trace Element Analysis by Spectroscopy Method, Faculty of Chemistry, Adam Mickiewicz University in Poznan, Umultowska 89b, 61-614 Poznan, Poland

[b] Clinic of Geriatric Dentistry, Karol Marcinkowski University of Medical Sciences in Poznań, Bukowska 70, 60-812 Poznan, Poland

ARTICLE INFO

Keywords:
LA-ICP-MS
Soft tissues
Implants
Elemental analysis
Quantitative analysis
Method validation

ABSTRACT

A new procedure for determination of elements derived from titanium implants and physiological elements in soft tissues by laser ablation inductively coupled plasma mass spectrometry (LA-ICP-MS) is presented. The analytical procedure was developed which involved preparation of in-house matrix matched solid standards with analyte addition based on certified reference material (CRM) MODAS-4 Cormorant Tissue. Addition of gelatin, serving as a binding agent, essentially improved physical properties of standards. Performance of the analytical method was assayed and validated by calculating parameters like precision, detection limits, trueness and recovery of analyte addition using additional CRM - ERM-BB184 Bovine Muscle. Analyte addition was additionally confirmed by microwave digestion of solid standards and analysis by solution nebulization ICP-MS. The detection limits are in range 1.8 μg g^{-1} to 450 μg g^{-1} for Mn and Ca respectively. The precision values range from 7.3% to 42% for Al and Zn respectively. The estimated recoveries of analyte addition line within scope of 83%–153% for Mn and Cu respectively. Oral mucosa samples taken from patients treated with titanium dental implants were examined using developed analytical method. Standards and tissue samples were cryocut into 30 μm thin sections. LA-ICP-MS allowed to obtain two-dimensional maps of distribution of elements in tested samples which revealed high content of Ti and Al derived from implants. Photographs from optical microscope displayed numerous particles with μm size in oral mucosa samples which suggests that they are residues from implantation procedure.

1. Introduction

Several analytical techniques had been applied to assess the content and distribution of metallic particles originated from implants in the tissue samples, including PIXE [1,2], scanning electron microscopy (SEM) combined with back-scattered electron imaging and energy dispersive X-ray spectroscopy [3], transmission electron microscopy (TEM) [4,5], synchrotron-radiation XRF [6], μXRF [7] and LIBS [8–10]. Yet, the most versatile and widely used method is laser ablation inductively coupled plasma mass spectrometry (LA-ICP-MS) due to the multielemental mapping capabilities with good spatial resolution in low μm to hundreds μm range, low detection limits in sub μg g^{-1} levels and wide dynamic range [11]. LA-ICP-MS method allow to quantitatively analyze the tissue in bulk or thin sections placed on various bases and present the results in the form of 2D maps of content and distribution of elements in the sample [12–14]. Many articles regarding LA-ICP-MS analysis of tissue specimens were published in recent years. An organ which is most frequently investigated is the brain, both from human and animal donors. It was concluded that distribution of elements in brain is affected due to Parkinson's disease [15,16], Alzheimer's disease [17,18], tumors [19–21] and Wilson's disease [22,23]. Many other organs affected with illness were examined, such as liver [24–26], teeth [27–29], blood vessels [30], kidneys [31–34], eye lens [35], cartilage [36,37] and many more.

The LA-ICP-MS method was also used to investigate the influence of metallic objects, including implants, on the surrounding tissues. After inserting of an metallic object into the body of living animal and investigating tissues that were in direct contact, the elevated content of metallic elements was observed [38–40]. Studies were also performed on the tissues taken from patients with metallic implants which resulted in presence of metallic particles and elevated content of elements (Ti, Al, V, Mg) derived from implants [41–43].

* Corresponding author.
E-mail address: danutaba@amu.edu.pl (D. Barałkiewicz).

http://dx.doi.org/10.1016/j.talanta.2017.07.058
Received 14 June 2017; Received in revised form 19 July 2017; Accepted 20 July 2017
Available online 21 July 2017

For the quantification purpose a suitable calibration approach must be developed and validated since there are currently no standards or reference materials dedicated for elemental analysis in soft tissues by LA-ICP-MS or other techniques for direct solid sample analysis. The basic premise for the calibration approach is the production of series of solid standards with a matrix composition and structure similar to the analyzed sample and spiking them with analyte and designating the element with uniform distribution in the sample as an internal standard. Several approaches based on matrix matched standards were suggested and successfully applied with the most popular using homogenized tissue spiked with analyte, since the matrix is practically identical in sample and standards [44–46]. Other methods worth mentioning are pressed pellets of powder material (usually reference materials or synthetic matrix) or embedding into polymer resin [47]. It is possible to introduce analyte solution along with the sample aerosol directly into the plasma, thus avoiding preparation of standards with matrix similar to the test sample [48]. Also, several calibration strategies were proposed which were based on non-matrix matched standards, e.g. using spiked agarose and gelatin [49,50], spin coating with PMMA film containing analytes [51], ablation of dried droplets [52] or preparing patterns printed with analyte solution on paper or other medium [53].

Instrumental methods in general are widely used in all imaginable purposes and measurements, including in medicine, environmental and forensic sciences. However, vast majority of them, including LA-ICP-MS, are comparable methods which require calibration and using standards. In order to verify the reliability of measurement results, an analytical procedure should be validated according to the principles of metrology which require certain parameters of the analytical method to be assessed. The parameters include selectivity, limit of detection, precision, reproducibility, working range, linearity and trueness, often expressed as recovery [54]. The last parameter is of critical importance and requires the reference materials with known analyte content in order to check if the measured analytical signal is in accordance with the actual analyte content. The purpose of validation is to provide evidence that the developed and applied analytical method is fit for intended use by testing the abovementioned important parameters.

In this work, the quantitative analysis of human oral mucosa samples by LA-ICP-MS in the form of maps with distribution of elements are presented. In order to achieve this the following steps were accomplished: i) tissue samples were collected from patients with titanium based dental implants, ii) preparation of analytical procedure for in situ determination of Ti, Al and physiological elements (Ca, Mg, Zn, Cu, Fe, Mn), iii) validation of analytical procedure, iv) application of developed procedure to the real samples.

2. Materials and methods

2.1. Samples

The analyzed tissue samples were fragments of oral mucosa collected from patients undergoing the implantation procedure. The samples under investigation were fragments of oral mucosa from the alveolar ridge covering a two-stage, intraosseous, screw-type titanium implant. The applied implants were made of grade 4 pure titanium containing 99% Ti. The implant system consists of an intraosseous implant and temporary cover screw. The intraosseous implant is directly inserted into the bone and has the porous structure in order to improve osseointegration. The porosity of implant is enhanced by sandblasting with Al oxide aerosol [55,56]. Phases of clinical procedures were conducted with the approval of the Bioethics Committee of the Poznan University of Medical Science. All study participants provided written informed consent for the collection of tissues. Prior to the implantation procedure the fragment of the mucous membrane covering the alveolar ridge, the planned bed around the implant, was collected and served as a control group. Mucous membrane sample from oral cavity was taken during revealing of the implant after 3–5 months healing period when the implant is osseointegrating with the bone tissue. Unveiling was performed carefully using a surgical stainless steel scalpel. Directly after incision the slices of oral mucosa were carefully rinsed with demineralized water and stored in the polypropylene microtubes (Sarstedt) in −18 °C, so as to inhibit biological decay, until further treatment. The oral mucosa samples were thawed in room temperature, immersed in cooling medium (OCT Embedding matrix, CellPath) and cut into 30 μm thin sections using cryostat (Leica CM 1850) at −18 °C, placed on the Polyethylene terephthalate (PET) base and stored in −18 °C until further analysis. Prior to the LA-ICP-MS analysis sample sections were dried in air in room temperature and photographed using optical microscope. The microscopic images of tissue samples were compared with the maps of distribution of elements obtained by the LA-ICP-MS.

2.2. Instrumentation

An LA system (LSX-500, CETAC Technologies, USA) with a quadrupole ICP-MS (Elan DRC II, Perkin-Elmer Sciex, Canada) was used in the experiment. The instrumentation was optimized on the daily basis by ablating the standard reference glass material NIST SRM 610 and adjusting the nebulizer gas flow, RF generator power and ion lens voltage in order to obtain the maximum signal intensity for $^{24}Mg^{+}$, $^{115}In^{+}$, $^{238}U^{+}$ and to control and maintain the ratio of oxide $^{232}Th^{16}O^{+}/^{232}Th^{+} < 0.2\%$ and doubly charged ions $^{42}Ca^{2+}/^{42}Ca^{+} < 0.5\%$. The following isotopes were measured throughout all experiments: ^{27}Al, ^{43}Ca, ^{63}Cu, ^{57}Fe, ^{26}Mg, ^{55}Mn, ^{31}P, ^{49}Ti and ^{66}Zn. ^{13}C and ^{34}S were measured to check their usefulness as the internal standard. The parameters of laser ablation system were selected so as to obtain the desirable spatial resolution of LA images and sufficiently high signal intensities and to ensure that the whole thin section of sample and standard was ablated. The diameter of laser beam was arbitrary set to 25 μm based on previous experiments. The optimization of scanning speed, repetition rate and laser energy was performed by ablating a thin section of 50 μg g^{-1} standard in order to obtain compromise

Table 1
Operating conditions for LA-ICP-MS system.

Laser ablation		ICP-MS	
Instrument	CETAC LSX-500, Nd-YAG	Instrument	PE Sciex ELAN 6100 DRC II
Wavelength [nm]	266	Nebulizer gas flow [L min^{-1}]	1.10–1.15
Pulse duration [ns]	5	Auxiliary gas flow [L min^{-1}]	1.2
Ablation frequency [Hz]	10	Plasma gas flow [L min^{-1}]	16
Spot size [μm]	25	RF Power [W]	1100–1150
Laser energy [mJ]	5.4	Lens setting	Autolens calibrated
Scan rate [μm s^{-1}]	100	Detector mode	Dual (pulse counting and analog mode)
Distance between scan lines [μm]	25	Internal standard	^{34}S
Scan method	Mapping 2D	Dwell time: isotope/[ms]	$^{31}P/10$, ^{13}C,^{26}Mg,^{55}Mn,^{63}Cu,$^{66}Zn/20$, $^{57}Fe/30$, ^{27}Al,^{34}S,$^{43}Ca/50$, $^{49}Ti/100$
Carrier gas	Ar	Sweeps	1

between good spatial resolution of images and overall time of analysis. Due to the relatively high content of Sb in PET base ^{121}Sb served as an element indicating that the analyzed thin section was completely ablated. The instrumental parameters are presented in Table 1. In order to generate images of elemental distribution samples and standards sections were completely ablated by laser beam traversing in a rectangular pattern composed of parallel lines of the same length, line by line with the direction from left to right side of the sample and with 3 s delay at the end of each line. The width of the ablation line and the distance between the centers of the lines was set to 25 μm. Number and length of scan lines were set individually for each sample. Microsoft Excel 2010 was used as data treatment software and OriginLab Pro 2016 for making 2D contour plots. Photographs of samples were taken using an optical stereoscopic microscope. During LA of areas of the sample with very high content of analytes a tailing effect may occur due to prolonged washout time [38]. The conditions responsible for this are: huge difference in signal intensities (several orders of magnitude) of the ablated adjacent areas, too large volume of the ablation chamber, the length of tubing, too large scanning speed of the sample and too low carrier gas flow. In the experiment the volume of standard ablation chamber was reduced from 78 mL to 31 mL by elevating the PTFE support for the sample which significantly reduced tailing effects and washout times of the aerosol resulting in better defined LA images. The comparison of single ablation line of NIST 610 CRM in the original and modified ablation chamber are presented in Fig. S.1 in Supplementary material. The microwave digestion system (Ethos One, Milestone, Italy) was used for solid standards digestion. Solutions obtained after digestion were analyzed by an solution nebulization ICP-MS (SN-ICP-MS) (Elan DRC II, Perkin-Elmer Sciex, Canada) equipped with a quartz injector and cyclonic spray chamber in order to confirm the proper analyte addition.

2.3. Preparation of standards

In order to obtain quantitative data the calibration approach based on matrix matched solid standards with analyte addition was used. The matrix material was pulverized cormorant tissue MODAS-4 CormTis (Consortium MODAS, Poland) which is a polish CRM with certified and informative values of content for selected elements. In order to improve coherence of solid standards a gelatin powder (Gelatin, European Pharmacopeia grade, VWR Chemicals) was added as a binding medium and matrix material since its composition is mostly animal proteins, collagen and elastin. Cormorant tissue and gelatin have similar composition to the analyzed oral mucosa which assured the similar behavior of standards and tissue during LA. Moreover, addition of gelatin critically improved mechanical properties and behavior of cormorant tissue during the preparation of thin sections. All standards were prepared by accurately weighing 200 mg of cormorant tissue powder and 100 mg of gelatin powder on the analytical balance (Kern ABJ, Germany). Analyte solutions were prepared from 1000 mg L^{-1} and 10,000 mg L^{-1} single element stock solutions (Ti, Al, Mg, Ca, Fe, Zn, Cu, Mn; Certipur, Merck) in demineralized water (Smart2Pure, TKA Water Purification Systems, Germany) with addition of conc. HNO_3 (Suprapur, Sigma-Aldrich) to obtain ca. 2.5% acid concentration in all analyte solutions. To the weighed portion of gelatin in agate mortar 300 μL of analyte solution was added and mixed to ensure that all gelatin absorbed the solution. After that, the weighed portion of dry cormorant tissue powder was added and mixed thoroughly to form well homogenized pulp which was immediately frozen in −18 °C in order to minimize water loss and stored until cryocutting. The blank standard was prepared with addition of 2.5% HNO_3 to the dry matrix material. Frozen solid standards were cryocut in the same manner as the tissue samples. All standards were prepared in duplicate for the microwave digestion. Solid standards with following analyte content in μg g^{-1} were prepared: Ti, Al (5, 20, 50, 100, 400); Mg, Ca (300, 500, 1000, 3000); Fe, Zn (20, 50, 300); Cu, Mn (1, 5, 20, 50, 100, 200). Standards for trueness and recovery assessment were prepared similarly to cormorant muscle based calibration standards using different CRM - ERM-BB184 Bovine Muscle, with addition of Ti and Al and elements with certified or informative content (Mg, Ca, Fe, Zn, Cu and Mn).

2.4. Microwave digestion

In order to confirm that solid standards were prepared properly and the signals obtain by LA-ICP-MS correspond to the actual analyte addition standards were mineralized in the microwave assisted high pressure digestion system. Directly after addition of analyte solution to the powder matrix and preparation of the solid standard it was accurately weighed and immediately put into the quartz vessel with 0.5 mL conc. HNO_3 (Suprapur, Merck) and 0.5 mL conc·H_2O_2 (TraceSELECT, Fluka) to minimize water loss and placed in a sealed Teflon tube. The weighed portion of the sample was typically ca. 0.15 g. The heating program was performed in two steps: (1) ramp time 15 min, (2) hold time 25 min; maximal power 1100 W, maximal temperature 150 °C. The mineralized samples were quantitatively transferred into 10 mL volumetric vessels and filled with demineralized water and analyzed by SN-ICP-MS.

3. Results and discussion

3.1. Analytical method

The analyzed isotopes are theoretically hampered with polyatomic interferences forming in the argon plasma in ICP-MS, especially when elements with lower mass are abundant in sample matrix, i.e. H, C, N, O or Cl. In the argon plasma isotopes of those elements form polyatomic species with *m/z* ratio equal to the isotopes of interest [57]. Examples of the most probable interferences for measured *m/z* are gathered in Table S.1 in Supplementary Material. In order to check the influence of light matrix elements on signal intensity of analytes pure solid salts deposited on PET base and substances containing large amounts of N, C, O, Cl and P were ablated using the same LA parameters as for the tissue samples. The salts ablated were ammonium persulphate (> 98%, Sigma Aldrich), sodium chloride (99.99%, Merck), ammonium phosphate (> 99%, Sigma Aldrich), methionine and cysteine (> 98%, Sigma Aldrich). The results of experiment showed that only $^{27}Al^+$ and $^{55}Mn^+$ signals elevated slightly and irregularly and signals of the other analytes remained at the gas background level (see Fig. S.2 in Supplementary material). This suggests that polyatomic species with *m/z* of the analyzed elements are below detection capability of instrument and minor signals for *m/z* 27 and 55 might be due to the impurities present in salts. Cooling medium was analyzed by LA-ICP-MS in order to check for possible contamination. Signals of all analytes in cooling medium were at the same level as PET base, which is presented in Fig. S.3 in Supplementary material. LA-ICP-MS, like most of instrumental techniques, is a comparative method. Thus, in order to obtain quantitative results the analytical signal must be transformed to the values of content or concentration by establishing a calibration relationship between the analytical signal and the measurand. To achieve this goal calibration standards must be employed into the analytical method, such as thin sections of solid standards described herein. Currently, no standards or CRM based on soft tissues and dedicated for LA-ICP-MS are available in trade. Therefore, in-house calibration approach based on matrix matched standards with analyte addition was developed. In order to assure that the same mass is ablated, tissue samples and standards were cryocut into 30 μm thin sections using microtome. Attempts were made to cryocut thin sections of solid standards based on CRM powder with addition of analyte solution and surfactant Triton X-100 [43] in various ratios. However, it was impossible to achieve satisfying homogeneity, furthermore, slices of standard felt apart and crumbled during cryocutting. Therefore, the

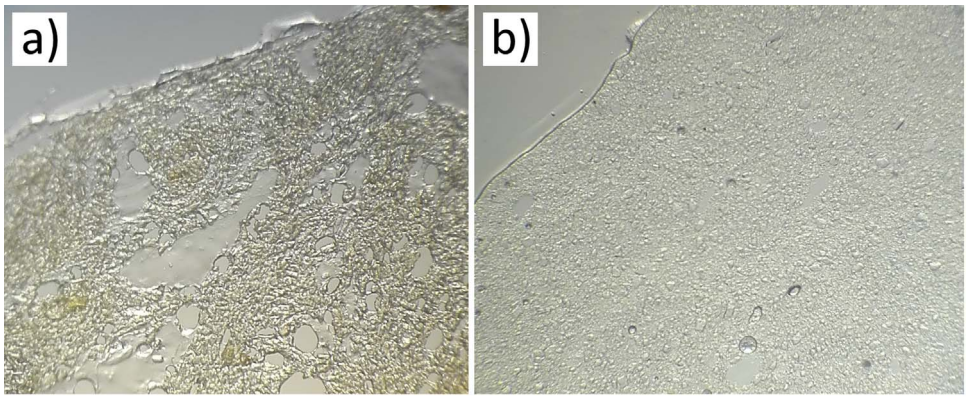

Fig. 1. Optical microscope photograph of thin sections of matrix matched solid standard: a) without binder addition, b) with addition of binder – gelatin. Addition of binding agent results in better homogeneity and coherence of standard and lower granularity in comparison to standard without binder.

binding agent was added which significantly improved coherence and homogeneity of standards and allowed for proper preparation of uniform thin sections. The microscope photographs of thin sections of standards without and with addition of gelatin are presented in Fig. 1. The ratio of CRM powder to gelatin powder masses is 2:1 in every calibration and blank standard, thus, the influence of gelatin on content of elements in CRM is constant in every standard.

Carbon is the main building element of proteins which are the main components of analyzed tissue and standards. However, it is also the most abundant element in PET which is the main component of the sample base. Both tissue and PET base are ablated simultaneously by the laser, yet not always in the same proportion. On the other hand, sulphur is not present in PET base in detectable amounts but is relatively abundant and homogenously distributed in the oral mucosa and solid standards, mainly as amino acids which build up proteins: methionine, cysteine and cystine. Two isotopes of sulphur (^{33}S and ^{34}S) were monitored during LA analysis. The ratio of ^{33}S and ^{34}S remained constant during measurements of samples and standards which showed that no detectable polyatomic interferences occurred which could affect the $^{33}S/^{34}S$ ratio. Isotope ^{34}S has higher abundance than ^{33}S (4.29% and 0.76% respectively), therefore, the isotope ^{34}S was selected as internal standard in further experiments. Sulphur isotopes were successfully applied as internal standards in analysis of other samples, e.g. hair, feathers and plant material [58–60]. Additionally, due to the formation of particle and gaseous fractions with different transportation efficiency, carbon is not recommended as the internal standard in tissue analysis by LA-ICP-MS [61].

Every calibration point was measured in five replicates, 1 min each, by ablating thin sections of solid standards and the mean value was used to construct the calibration curves. All LA-ICP-MS measurements were conducted ca. 10 min after sealing the sample/standard in ablation chamber in order to completely washout the air and stabilize background signal of analytes (gas blank). Background signal of internal standard was compared prior to and after the laser action in order to check for signal drifts; no significant signal drifts were noted. Average background signal measured directly prior to all measurements of standards and samples was subtracted. Calibration curves for elements contained in implants, Ti and Al, are presented in Fig. 2. The parameters of calibration curve of other analytes are gathered in Table 2.

3.2. Microwave assisted digestion of standards

In order to determine the actual content of analytes in the prepared solid standards they were digested and analyzed with complementary method of SN-ICP-MS. The results are presented as a comparison of analyte content by ablating the thin section of solid standards with analyte content in the solution after digestion of solid standard measured by SN-ICP-MS. The results are displayed in Fig. 3 in the form of a graph representing results of solutions analysis by SN-ICP-MS in the function of the analyte content in solid standards measured by LA-ICP-MS. Vertical and horizontals bar represent standard deviation (SD) of five replicates of SN-ICP-MS and LA-ICP-MS measurements respectively. Data show good correlation of results for the same sample obtained with two different analytical methods, which is expressed as a factor of determination > 0.98 for all measured elements.

3.3. Analysis of oral mucosa

In order to verify the qualitative composition of an implant, the intraosseous implant and cover screw were analyzed by LA-ICP-MS. The results are presented in Fig. S.4 in Supplementary material. Two locations on the implant were selected: (1) a screw-shaped part that is inserted directly into the bone and (2) an abutment, where the cover screw is inserted for the healing period. Also, the result of analysis of temporary cover screw, which is made of pure Ti and placed for 3–5 months until the implant revealing procedure, is presented. The LA analysis showed that the intraosseous part of implant (1) is made of Ti, however, with very high Al content which is a remnant of sandblasting of the implant surface with Al_2O_3 [56]. The abutment of implant (2) is made of pure Ti, so is the cover screw. All three parts are subjected to friction and mechanical forces during the implantation procedure which may lead to release of metallic particles to the surrounding tissues, oral mucosa and bone. The developed analytical method is suitable for analysis of a soft tissue, either human or animal, that was in contact with titanium implants. The possible ways to collect tissue samples are biopsy, cutting a fragment of tissue during or after implantation procedure or post-mortem. In the presented paper the collected mucosal membrane are the residue or excessive tissue which is cut out prior to insertion of implant or after the healing period which usually takes 3–5 months. It is not always necessary to cut the fragment of mucosa during operation. The decision is up to the person performing the procedure with regard to the individual case and the *primum non nocere* principle.

For comparison, the maps of control group samples are presented in Fig. 4 and Fig. S5 in Supplementary material in which the content of Ti and Al is much lower than in the sample after contact with implant. Oral mucosa thin sections were stained with haematoxylin and eosin (HE), which allowed to reveal the inner structure of the analyzed tissue. The maps of distribution of elements in this paper are representing the thin sections that were not stained with HE. The differences in the shape of a tissue sample photo and the maps of content of elements may be due to the fact that it was not always possible to obtain two consecutive thin sections of a sample of which one was ablated and other was HE stained/photographed. Maps of Ti and Al in oral mucosa

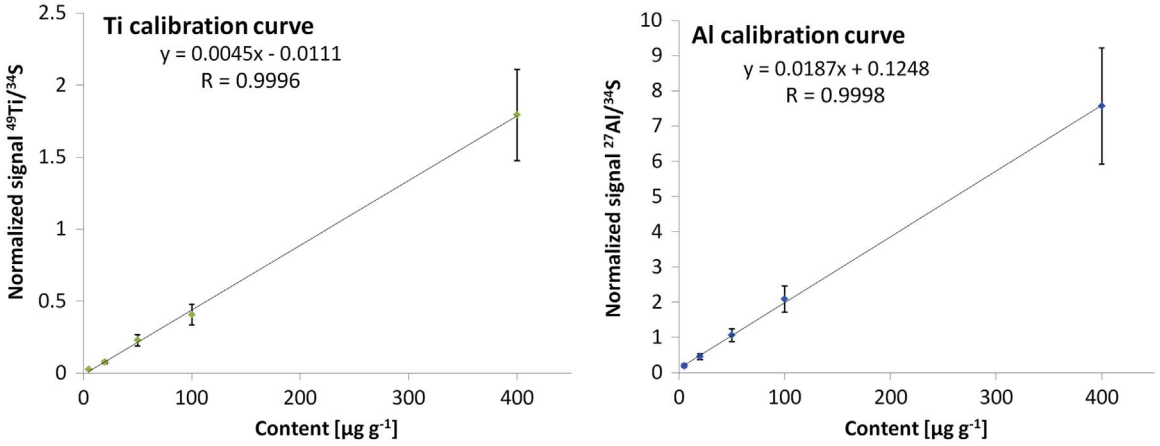

Fig. 2. Calibration curves for ^{49}Ti and ^{27}Al obtained by analysis of thin sections of matrix matched solid standards. Analytical signal of measured *m/z* is normalized by ^{34}S signal intensity; vertical bars represent standard deviation of mean signal of five replicates for each calibration point.

from patients after implantation revealed elevated content on small areas, usually on the edges of tissue thin section (see Fig. 5, Fig. 6 and Fig. S.6, Fig. S.7 in Supplementary material). The measured signals are very large and are located in spots with a small area, often with the width of single ablation line. Tailing effect in the direction of laser beam scan pattern is visible which is formed due to rapid change in content of analytes on very small areas. Responsible for this observation is the presence of metallic particles originated from dental implants and released during the implantation procedure. Very high content of Al in analyzed samples is caused by the presence of Al_2O_3 grit used for sandblasting of the intraosseous part of an implant in order to improve its porosity and osseointegration. Al_2O_3 remains in µm and sub-µm pores and crevices of the implant and may be released to the tissues during implantation procedure along with the titanium particles [56]. The particles containing Ti and Al remained in oral mucosa samples despite rinsing them with large amounts of demineralized water immediately after collection which suggests that the particles are imprinted in the tissue rather than just adhered to it. The particles that are larger than few µm are visible in the optical microscope as black points (see Fig. 6 and Fig S.7 in supplementary material). The

Table 2
Analytical parameters of calibration method based on the cormorant tissue standards.

Analytical parameter	Analyte addition	Ti	Al	Cu	Zn	Fe	Mn	Analyte addition	Mg	Ca
Standards range [µg g^{-1}]		5–400	5–400	1–200	20–300	20–300	1–100		300–3000	500–3000
Regression equation		y = 0.004494–0.0111	y = 0.01867 +0.1248	y = 0.00330 +0.0036	y = 0.00055 +0.0033	y = 0.000316 +0.01673	y = 0.01257–0.0211		y = 0.000358–0.0228	y = 0.0000721 +0.0124
SD of slope		0.000061	0.00020	0.000097	0.00015	0.000014	0.00034		0.000020	8.1E-7
SD of intercept		0.0129	0.0373	0.0089	0.0022	0.0025	0.0173		0.0324	0.0015
Linearity; R		0.9996	0.9998	0.9987	0.9993	0.9989	0.9989		0.9968	0.9999
IDL[µg g^{-1}]		14	4.1	2.4	18	43	1.8		14	450
MDL[µg g^{-1}]		21	14	6.5	61	98	4.7		419	1174
Single line precision [%]	**5 µg g^{-1}**	30.9	24.7	33.6	[b]	[b]	27.1	**500 µg g^{-1}**	21.0	27.4
	20 µg g^{-1}	27.9	18.4	31.5	41.6	35.1	22.8	**1000 µg g^{-1}**	21.4	23.7
	50 µg g^{-1}	21.0	16.7	21.2	30.7	26.3	17.1	**3000 µg g^{-1}**	21.7	22.7
	highest standard[a]	18.9	21.8	23.9	26.3	25.4	19.0			
Repeatability [%]	**5 µg g^{-1}**	17.9	9.2	16.7	14.5	21.9	16.6	**500 µg g^{-1}**	23.4	16.0
	20 µg g^{-1}	13.8	11.1	25.1	19.4	18.5	20.4	**1000 µg g^{-1}**	25.2	19.0
	50 µg g^{-1}	16.9	24.5	21.2	13.0	18.2	18.2	**3000 µg g^{-1}**	16.1	12.3
	highest standard[a]	17.7	18.9	17.6	14.0	14.7	17.7			
Intermediate precision [%]	**5 µg g^{-1}**	14.4	20.1	17.1	14.2	16.9	13.3	**500 µg g^{-1}**	23.2	15.7
	20 µg g^{-1}	12.3	19.2	9.6	9.4	10.7	14.7	**1000 µg g^{-1}**	20.8	11.2
	50 µg g^{-1}	11.7	13.1	11.0	11.4	10.8	11.1	**3000 µg g^{-1}**	17.5	12.3
	highest standard[a]	8.7	7.3	9.1	10.2	8.6	8.2			

[a] Ti, Al (400 µg g^{-1}), Cu (200 µg g^{-1}), Zn, Fe (300 µg g^{-1}), Mn (100 µg g^{-1}).
[b] spike to small.

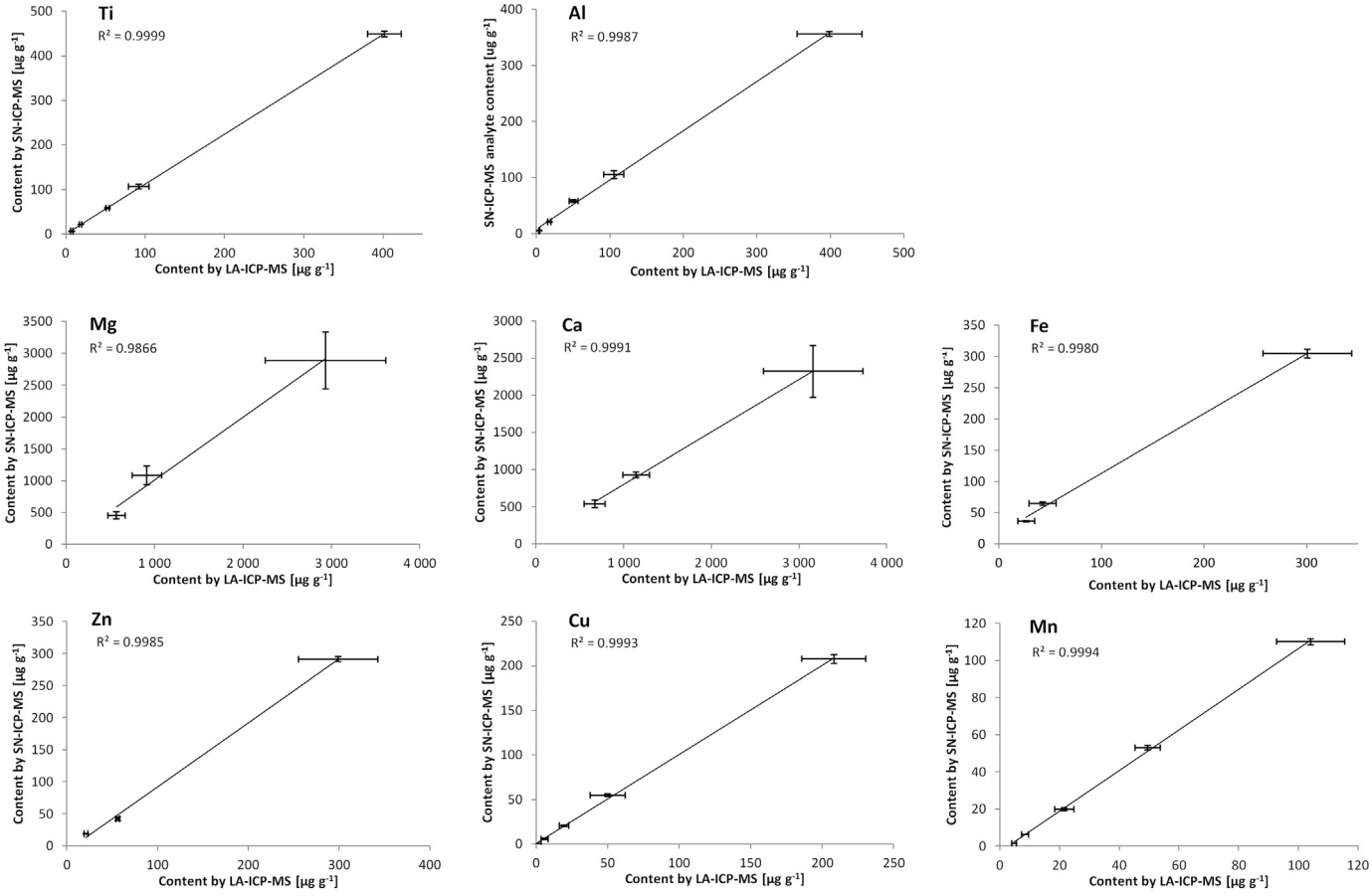

Fig. 3. Comparison of results obtained after direct analysis of the solid standards by LA-ICP-MS (x-axis) and after microwave assisted digestion of solid standards by SN-ICP-MS (y-axis). Horizontal and vertical bars represent SD of 5 measurement replicates of each standard by LA-ICP-MS and SN-ICP-MS respectively.

position of high Ti signals on maps are in good accordance with the position of black points on the photograph for the given sample. The distribution of building elements (C, S, P) in the maps is roughly uniform in all analyzed samples, but the distribution of the physiological elements (Mg, Ca, Fe, Zn, Cu, Mn) varies slightly depending on the origin of the sample (different patients), collection sites (incision depth) and degree of keratinization of the tissue.

In the Fig. 6 and Fig S.7 in Supplementary material local high signals of Ca, Mg and P with very sharp contour and irregular shape were measured in the analyzed oral mucosa samples. The areas with elevated Ca and P content have width in the order of tens to hundreds μm and were located usually on the edge of tissue. Those high signals were recorded only in oral mucosa tissues after the implantation procedure. This might be due to the microscopic bone splinters after drilling in the bone prior to implant insertion. An elevated content of Mg is observable along with the Ca and P, which are present in large amounts in bone tissue. Additionally, elevated content of Zn was recorded in the same areas as Ca, P and Mg. For comparison, the natural contents of P, Ca, Mg and Zn in human bone measured with different techniques are 79.7 g kg^{-1}, 183 g kg^{-1}, 2137 mg kg^{-1} and 90 mg kg^{-1} respectively [62]. Although samples were thoroughly rinsed with water the remnants of bone splinters remained on their surface. However, it is one of the functions of oral mucosa to form a protective barrier against chemical substances, foreign objects and mechanical damage thus protecting the deeper tissues and organs.

Titanium implants were introduced to the dental practice in 1960 and have earned a well-deserved fame for their usability and excellent biocompatibility [63]. The main advantages of Ti based implants are good osseointegration, wear resistance, biocompatibility, mechanical properties and low density which allow them to replace missing tooth for decades if properly inserted and maintained [64,65]. However, the forces exerting on the implant and the environment of oral cavity may cause the electrochemical corrosion of implant and release of ions and metallic particles of the implant surface, despite the protective Ti oxide layer [66]. The intraosseous part of implant have very high surface area and porosity, resembling the bone tissue, in order to stimulate osteoblasts to form new cells around the implant [66]. To increase the porosity implants are sandblasted with Al_2O_3 grit which remains in the pores and on the surface of an implant [56,67]. The implantation procedure require to drill a bone and to insert the implant, similarly as a screw, into the bone. Described factors may generate numerous metallic particles of nanometers to micrometers size which remain in the adjacent tissues, i.e. bones and oral mucous membranes [68]. Furthermore, nanoparticles and ionic species penetrate to the deeper tissues and the bloodstream where they may reach to more distant organs, like lymph nodes, lungs and spleen [68]. The release of metal ions and particles to the tissues may cause allergic reactions in patient leading to inflammation, implant rejection or systemic toxicity if in the case of defective implant, multiple implants or chronic exposure. Pure Ti and its alloys is considered safe and well tolerated, however, aforementioned adverse reactions may be enhanced due to the presence of other elements beside Ti, like aluminum and vanadium in commonly used Ti6Al4V alloy or trace levels of impurities to which a patient may be allergic (e.g. Ni, Cr, Co). The allergic reactions to Ti was recognized in 0.6% of 1500 patients in a clinical study [69]. It is possible that responsible for the failure if implant in human body are trace levels impurities in the titanium intraosseous implant. A good indicator of the excessive release of metals to the patient's body is blood analysis [70,71].

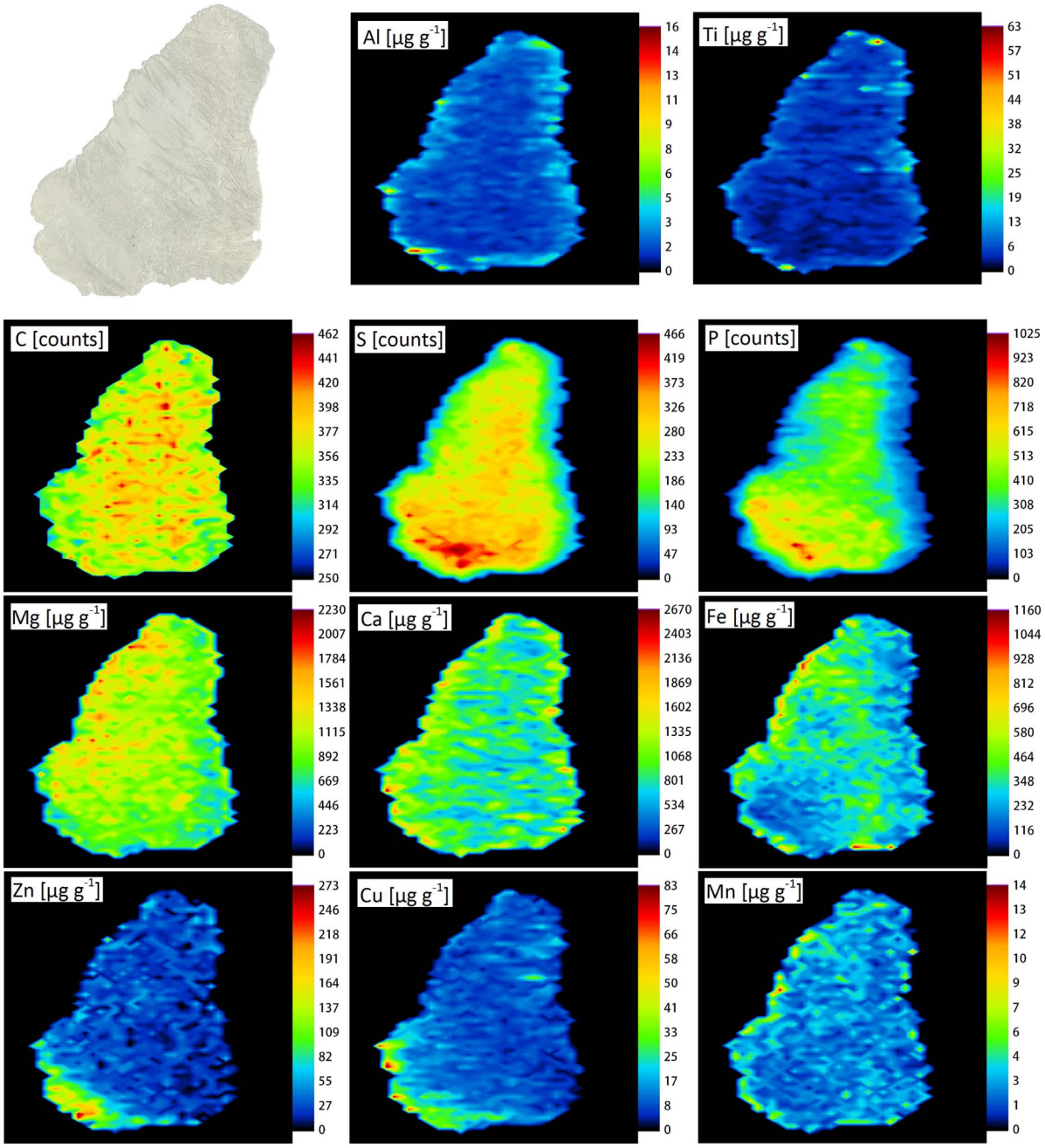

Fig. 4. Maps of distribution of Ti, Al, Mg, Ca, Fe, Zn, Cu and Mn in the oral mucosa sample of the control group. Ti and Al are present in low amounts in the control group sample.

3.4. Figures of merit

3.4.1. Precision

Precision of method is expressed by three parameters, depending on the time interval between the measurements. Each ablation run consist of multiple data points, whose number depends on the scanning speed and dwell times for each measured *m/z*, which altogether result in a single ablation line, for which mean value and SD can be calculated. All repetitions of single line ablations for each standard allows to calculate mean value and SD which is called short-time precision or repeatability. Combination of mean values from analyses performed over the span of several days contribute to the long-term precision or intermediate precision, which, in this work, is calculated for measurements on three consecutive days. The values of single line precision, repeatability and intermediate precision are presented in Table 2.

3.4.2. Limit of detection

Limit of detection was estimated according to the IUPAC method, namely as 3 SD of the blank signal. Two sources of blank signal were used which allowed to calculate two parameters: instrumental detection limit (IDL) and method detection limit (MDL). The former parameter refers to the minimal amount of analyte which can be reliably detected by the instrument, the latter parameter takes into consideration the analytical procedure by which standards were produced. IDL is estimated based on the background signal (gas blank) recorded when no standard or sample is ablated according to the equation: IDL = $3s_{gas}/a$, where s_{gas} – SD of background signal, a – slope of calibration curve. To estimate MDL a signal is measured that is expected to be the lowest of all calibration standards or the sample. Presumably, this signal is proportional to the natural content of analyte in a matrix material that comprise the blank and calibration standards. Also, steps of analytical procedure like homogenization, mixing,

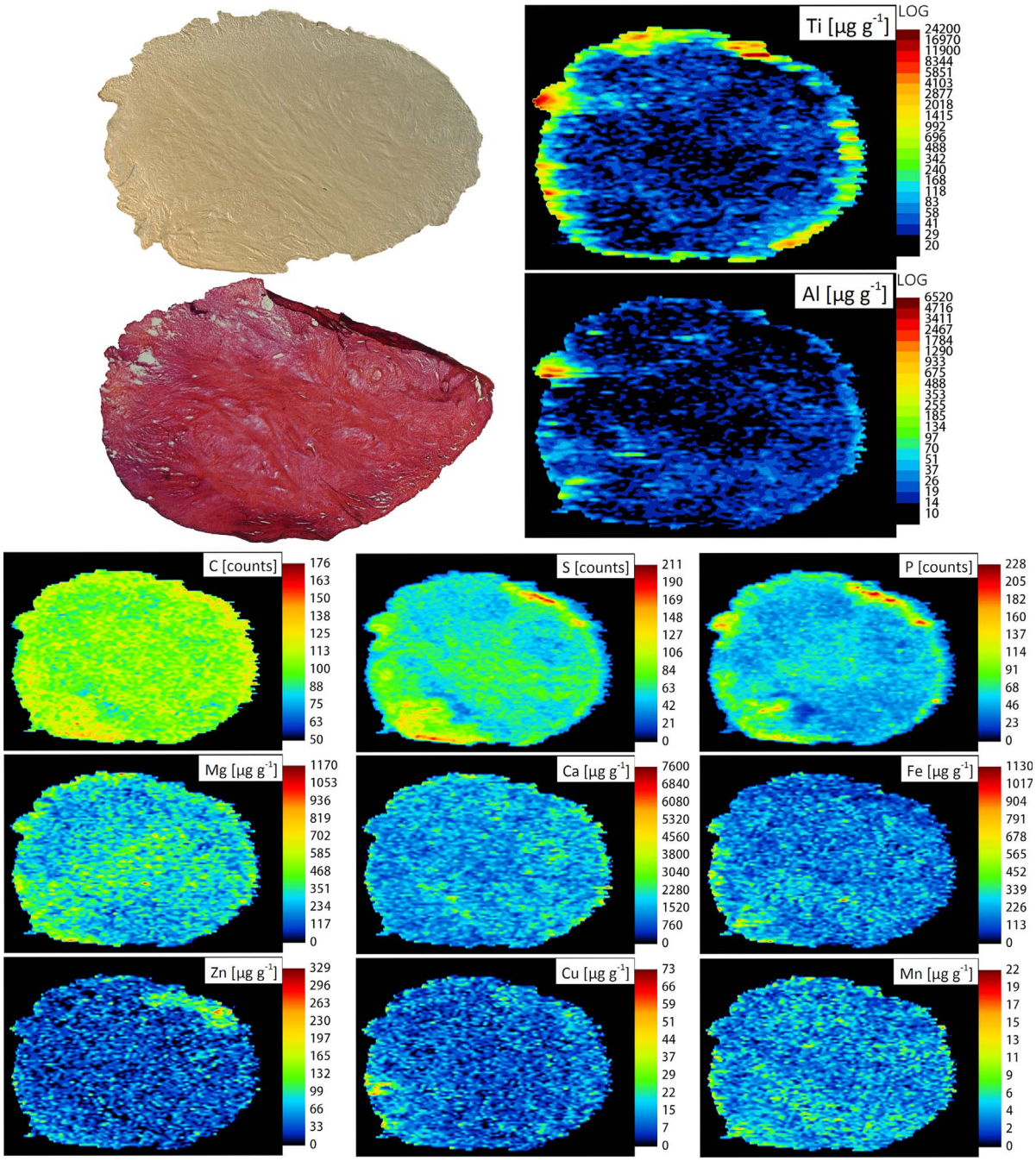

Fig. 5. Maps of distribution of Ti, Al, Mg, Ca, Fe, Zn, Cu and Mn in the oral mucosa sample collected from patient after implantation procedure. Elements derived from implants (Ti, Al), physiological (Mg, Ca, Fe, Zn, Cu, Mn) and building (C, S, P) elements of tissue and photographs of unstained oral mucosa and after HE staining are presented.

extraction, addition of binding agents or other chemical modifiers and possible interferences of the other matrix components may influence the content of analyte in standards and blank. A signal of blank standard was used in order to estimate MDL using the equation: MDL = $3s_{blank}/a$, where s_{blank} – SD of ablated standard with low analyte addition (i.e. lowest standard for particular analyte). The estimated values of IDL and MDL are presented in Table 2.

3.4.3. Recovery

Currently there are no CRMs with matrix similar to the analyzed tissues with certified content of Ti or Al on detectable levels by LA-ICP-MS. In order to assess the correctness of analyte addition to the matrix matched standards recoveries of analyte spike were estimated by analyzing a set of standards with a matrix based on ERM-BB184 Bovine Muscle with the calibration data (curve) based on standards made of MODAS-4 CormTis. In order to verify the recovery of added analyte content to the CRM a blank standard and a set of standards with analyte addition was prepared using solutions of Ti and Al and also elements whose content is stated as certified or informative in the CRM certificate. The value measured for blank standard was subtracted from the value measured for spiked standards in order to obtain the value of added analyte alone. The value of the recovery of spike was calculated using the equation: $R = (c\text{-}c_{cert})/c_{add}$, where c – measured value, c_{cert} – reference value from certificate, c_{add} –analyte addition. The obtained values of recovery of analyte addition, expressed in %, are gathered in Table 3.

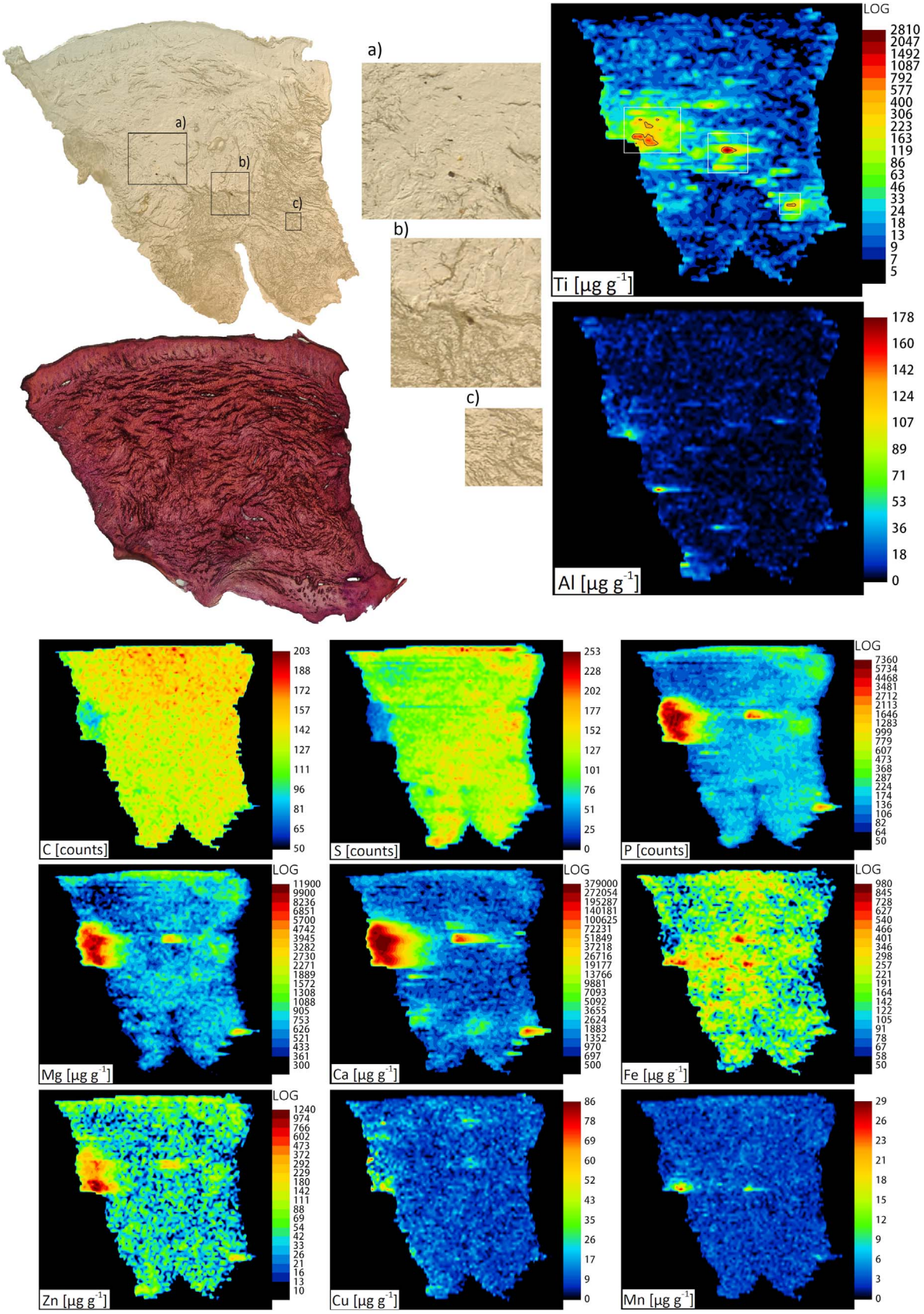

Fig. 6. Maps of distribution of Ti, Al, Mg, Ca, Fe, Zn, Cu and Mn in the oral mucosa sample collected from patient after implantation procedure. Elements derived from implants are Ti and Al. A distribution of physiological and building elements of oral mucosa and photographs after HE staining and unstained are presented. Elevated content of elements (P, Ca, Mg, Zn) derived from bone splinters remaining after drilling is shown. Close-ups of areas with visible particles are provided.

Table 3
Recoveries of analyte addition to the matrix-matched standards based on ERM-BB184 Bovine Muscle with calibration based on MODAS-4 CormTis matrix material.

Parameter	Analyte spike	Ti	Al	Cu	Zn	Fe	Mn	Analyte spike	Mg	Ca
Content [μg g^{-1}]	**5 μg g^{-1}**	[a]	7.2	7.7	[b]	[b]	4.5	**500 μg g^{-1}**	586	641
Recovery [%]		[a]	144	153	[b]	[b]	91		117	128
Content [μg g^{-1}]	**20 μg g^{-1}**	18.5	18.8	19.4	27.8	[b] 37.3	18.3	**1000 μg g^{-1}**	939	1082
Recovery [%]		93	94	97	139	[b] 187	91		94	108
Content [μg g^{-1}]	**50 μg g^{-1}**	50.6	50.2	67.3	42.2	53	41.3	**3000 μg g^{-1}**	3020	2973
Recovery [%]		101	101	135	84	107	83		101	99
Content [μg g^{-1}]	**highest standard**[a]	413	391	232	298	292	102			
Recovery [%]		103	98	116	99	97	102			

[a] Ti, Al (400 μg g^{-1}), Cu (200 μg g^{-1}), Zn, Fe (300 μg g^{-1}), Mn (100 μg g^{-1}).
[b] spike too small.

Table 4
Trueness values for elements with certified or informative content in ERM-BB184 Bovine Muscle.

		Mg	Ca	Fe	Zn	Cu
Bovine muscle	Certified value [μg g^{-1}]	1000[a]	155[a]	75 ± 4	146 ± 7	2.31 ± 0.09
	Measured value [μg g^{-1}]	875 ± 115	168 ± 51	83 ± 26	192 ± 47	3.29 ± 0.41
	Trueness [%]	87.5	108.5	110.0	131.8	142.3

[a] informative value.

3.4.4. Trueness

The trueness of developed analytical method was assessed by comparing certified values for given CRM with measured values which is presented in Table 4. The extrapolation method of calibration curve was used; the standard with no analyte addition (blank) was set to c = 0 μg g^{-1} on a calibration curve, which was built on standards based on CRM with multiple analyte addition, and the actual content of analyte was given by equation: c = intercept/slope. Standards based on ERM-BB184 Bovine Muscle material were verified for the certified and informative analyte content of Fe, Zn, Cu, Mg*, Ca*, where "*" – informative value. Values of certified and measured content for analyzed elements are in acceptable agreement. The certified content for Mn was too low to properly quantify its content in CRM and calculate the trueness values (0.276 μg g^{-1}).

4. Conclusions

In this work, the analytical procedure of quantitative analysis of clinical soft tissues by LA-ICP-MS was developed. To accomplish this a series of matrix matched solid standards with analyte addition based on the pulverized cormorant tissue as the matrix material was prepared in the form of thin sections. Addition of gelatin significantly improved the physical properties of standards during cryocutting. Validation of analytical parameters, such as limits of detection, trueness, recovery and precision, was performed in order to confirm the usefulness of the analytical method in the determination of physiological elements and derived from metallic implant in soft tissues. The values of trueness for certified elements in analyzed CRMs are in the range 74%–142%. The validated procedure was applied to the thin sections of human oral mucosa that was in direct contact with metallic implants and results were presented in the form of two-dimensional maps of content of Ti, Al and physiological elements. Obtained maps revealed that Ti is abundantly present in the oral mucosa, mainly in the form of metallic particles which are remnants of the drilling procedure and after the insertion of implant in the patient's bone. The content of physiological elements, which are present naturally in the tissue, i.e. Ca, Mg, Fe, Zn, Cu and Mn was also measured. The developed method can be applied to other types of clinical and animal soft tissues allowing to examine the distribution of elements in thin cross sections of tested samples with spatial resolution of 10 × 25 μm^2, determined by LA parameters.

Acknowledgements

This work was financially supported by the Research Project of the National Science Centre Poland (2015/17/N/ST4/03808).

The authors would like to thank dr hab. Lucyna Mrówczyńska (Department of Cell Biology, Faculty of Biology, Adam Mickiewicz University in Poznań) for histological preparation of tissues samples.

Appendix A. Supplementary material

Supplementary data associated with this article can be found in the online version at doi:10.1016/j.talanta.2017.07.058.

References

[1] G.P. Buso, S. Galassini, G. Moschini, P. Passi, A. Zadro, N.M. Uzunov, B.L. Doyle, P. Rossi, P. Provencio, PIXE microbeam analysis of the metallic debris release around endosseous implants, Nucl. Instrum. Methods Phys. Res. Sect. B Beam Interact. Mater. At. 240 (2005) 91–94. http://dx.doi.org/10.1016/j.nimb.2005.06.094.
[2] S. Novak, D. Drobne, J. Valant, P. Pelicon, Internalization of consumed TiO2 nanoparticles by a model invertebrate organism, J. Nanomater. 2012 (2012). http://dx.doi.org/10.1155/2012/658752.
[3] M. Topolovec, I. Milošev, A. Cör, R. Bloebaum, Wear debris from hip prostheses characterized by electron imaging, Open Med. 8 (2013) 476–484. http://dx.doi.org/10.2478/s11536-013-0156-7.
[4] P.F. Doorn, P.A. Campbell, J. Worrall, P.D. Benya, H.A. McKellop, H.C. Amstutz, Metal wear particle characterization from metal on metal total hip replacements: transmission electron microscopy study of periprosthetic tissues and isolated particles, J. Biomed. Mater. Res. 42 (1998) 103–111. http://dx.doi.org/10.1002/(SICI)1097-4636(199810)42:1<103::AID-JBM13>3.0.CO;2-M.
[5] J. Soto-Alvaredo, E. Blanco, J. Bettmer, D. Hevia, R.M. Sainz, C. López Cháves, C. Sánchez, J. Llopis, A. Sanz-Medel, M. Montes-Bayón, Evaluation of the biological effect of Ti generated debris from metal implants: ions and nanoparticles, Metallomics 6 (2014) 1702. http://dx.doi.org/10.1039/C4MT00133H.
[6] C. Carlier, B. Laforce, S.J.M. Van Malderen, F. Gremonprez, R. Tucoulou, J. Villanova, O. De Wever, L. Vincze, F. Vanhaecke, W. Ceelen, Nanoscopic tumor tissue distribution of platinum after intraperitoneal administration in a xenograft model of ovarian cancer, J. Pharm. Biomed. Anal. 131 (2016) 256–262. http://dx.doi.org/10.1016/j.jpba.2016.09.004.
[7] O. Hachmöller, A.G. Buzanich, M. Aichler, M. Radtke, D. Dietrich, K. Schwamborn, L. Lutz, M. Werner, M. Sperling, A. Walch, U. Karst, Elemental bioimaging and speciation analysis for the investigation of Wilson's disease using μXRF and XANES, Metallomics 8 (2016) 648–653. http://dx.doi.org/10.1039/C6MT00001K.
[8] S. Moncayo, F. Trichard, B. Busser, M. Sabatier-Vincent, F. Pelascini, N. Pinel, I. Templier, J. Charles, L. Sancey, V. Motto-Ros, Multi-elemental imaging of paraffin-embedded human samples by laser-induced breakdown spectroscopy, Spectrochim. Acta Part B At. Spectrosc. 133 (2017) 40–44. http://dx.doi.org/10.1016/j.sab.2017.04.013.
[9] M. Bonta, J.J. Gonzalez, C.D. Quarles, R.E. Russo, B. Hegedus, A. Limbeck, Elemental mapping of biological samples by the combined use of LIBS and LA-ICP-MS, J. Anal. At. Spectrom. 31 (2016) 252–258. http://dx.doi.org/10.1039/C5JA00287G.
[10] L. Sancey, V. Motto-Ros, B. Busser, S. Kotb, J.M. Benoit, A. Piednoir, F. Lux, O. Tillement, G. Panczer, J. Yu, Laser spectrometry for multi-elemental imaging of biological tissues, Sci. Rep. 4 (2014) 6065. http://dx.doi.org/10.1038/srep06065.
[11] B. Hattendorf, C. Latkoczy, D. Günther, Peer reviewed: laser ablation-ICPMS, Anal.

Chem. 75 (2003) 341 A–347 A. http://dx.doi.org/10.1021/ac031283r.
[12] J.S. Becker, M. Zoriy, A. Matusch, B. Wu, D. Salber, C. Palm, J.S. Becker, Bioimaging of metals by laser ablation inductively coupled plasma mass spectrometry (LA-ICP-MS), Mass Spectrom. Rev. 29 (2010) 156–175. http://dx.doi.org/10.1002/mas.20239.
[13] D. Pozebon, V. Dressler, G.L. Scheffler, Recent applications of laser ablation inductively coupled plasma mass spectrometry (LA-ICP-MS) for biological sample analysis: a follow-up review, J. Anal. At. Spectrom. (2017) 890–919. http://dx.doi.org/10.1039/C7JA00026J.
[14] I. Konz, B. Fernández, M.L. Fernández, R. Pereiro, A. Sanz-Medel, Laser ablation ICP-MS for quantitative biomedical applications, Anal. Bioanal. Chem. 403 (2012) 2113–2125. http://dx.doi.org/10.1007/s00216-012-6023-6.
[15] A. Matusch, C. Depboylu, C. Palm, B. Wu, G.U. Höglinger, M.K.H. Schäfer, J.S. Becker, Cerebral bioimaging of Cu, Fe, Zn, and Mn in the MPTP mouse model of Parkinson's disease using laser ablation inductively coupled plasma mass spectrometry (LA-ICP-MS), J. Am. Soc. Mass Spectrom. 21 (2010) 161–171. http://dx.doi.org/10.1016/j.jasms.2009.09.022.
[16] D. Hare, B. Reedy, R. Grimm, S. Wilkins, I. Volitakis, J.L. George, R.A. Cherny, A.I. Bush, D.I. Finkelstein, P. Doble, Quantitative elemental bio-imaging of Mn, Fe, Cu and Zn in 6-hydroxydopamine induced Parkinsonism mouse models, Metallomics 1 (2009) 53–58. http://dx.doi.org/10.1039/B816188G.
[17] R.W. Hutchinson, A.G. Cox, C.W. McLeod, P.S. Marshall, A. Harper, E.L. Dawson, D.R. Howlett, Imaging and spatial distribution of β-amyloid peptide and metal ions in Alzheimer's plaques by laser ablation-inductively coupled plasma-mass spectrometry, Anal. Biochem. 346 (2005) 225–233. http://dx.doi.org/10.1016/j.ab.2005.08.024.
[18] D.J. Hare, E.P. Raven, B.R. Roberts, M. Bogeski, S.D. Portbury, C.A. McLean, C.L. Masters, J.R. Connor, A.I. Bush, P.J. Crouch, P.A. Doble, Laser ablation-inductively coupled plasma-mass spectrometry imaging of white and gray matter iron distribution in Alzheimer's disease frontal cortex, Neuroimage 137 (2016) 124–131. http://dx.doi.org/10.1016/j.neuroimage.2016.05.057.
[19] M. Dehnhardt, M.V. Zoriy, Z. Khan, G. Reifenberger, T.J. Ekström, J. Sabine Becker, K. Zilles, A. Bauer, Element distribution is altered in a zone surrounding human glioblastoma multiforme, J. Trace Elem. Med. Biol. 22 (2008) 17–23. http://dx.doi.org/10.1016/j.jtemb.2007.08.002.
[20] M.V. Zoriy, M. Dehnhardt, A. Matusch, J.S. Becker, Comparative imaging of P, S, Fe, Cu, Zn and C in thin sections of rat brain tumor as well as control tissues by laser ablation inductively coupled plasma mass spectrometry, Spectrochim. Acta - Part B At. Spectrosc. 63 (2008) 375–382. http://dx.doi.org/10.1016/j.sab.2007.11.030.
[21] J.S. Becker, M.V. Zoriy, M. Dehnhardt, C. Pickhardt, K. Zilles, Copper, zinc, phosphorus and sulfur distribution in thin section of rat brain tissues measured by laser ablation inductively coupled plasma mass spectrometry: possibility for small-size tumor analysis, J. Anal. At. Spectrom. 20 (2005) 912. http://dx.doi.org/10.1039/b504978b.
[22] S. Boaru, U. Merle, R. Uerlings, A. Zimmermann, S. Weiskirchen, A. Matusch, W. Stremmel, R. Weiskirchen, Simultaneous monitoring of cerebral metal accumulation in an experimental model of Wilson's disease by laser ablation inductively coupled plasma mass spectrometry, BMC Neurosci. 15 (2014) 98. http://dx.doi.org/10.1186/1471-2202-15-98.
[23] O. Hachmöller, A. Zibert, H. Zischka, M. Sperling, S.R. Groba, I. Grünewald, E. Wardelmann, H.H.-J. Schmidt, U. Karst, Spatial investigation of the elemental distribution in Wilson's disease liver after d -penicillamine treatment by LA-ICP-MS, J. Trace Elem. Med. Biol. 44 (2017) 26–31. http://dx.doi.org/10.1016/j.jtemb.2017.05.008.
[24] A. Kindness, Two-dimensional mapping of copper and zinc in liver sections by laser ablation-inductively coupled plasma mass spectrometry, Clin. Chem. 49 (2003) 1916–1923. http://dx.doi.org/10.1373/clinchem.2003.022046.
[25] O. Hachmöller, M. Aichler, K. Schwamborn, L. Lutz, M. Werner, M. Sperling, A. Walch, U. Karst, Element bioimaging of liver needle biopsy specimens from patients with Wilson's disease by laser ablation-inductively coupled plasma-mass spectrometry, J. Trace Elem. Med. Biol. 35 (2016) 97–102. http://dx.doi.org/10.1016/j.jtemb.2016.02.001.
[26] P. M-M, R. Weiskirchen, N. Gassler, A.K. Bosserhoff, J.S. Becker, Novel bioimaging techniques of metals by laser ablation inductively coupled plasma mass spectrometry for diagnosis of fibrotic and cirrhotic liver disorders, PLoS One 8 (2013). http://dx.doi.org/10.1371/journal.pone.0058702.
[27] D. Kang, D. Amarasiriwardena, A.H. Goodman, Application of laser ablation-inductively coupled plasma-mass spectrometry (LA-ICP-MS) to investigate trace metal spatial distributions in human tooth enamel and dentine growth layers and pulp, Anal. Bioanal. Chem. 378 (2004) 1608–1615. http://dx.doi.org/10.1007/s00216-004-2504-6.
[28] A. Hanć, A. Olszewska, D. Barałkiewicz, Quantitative analysis of elements migration in human teeth with and without filling using LA-ICP-MS, Microchem. J. 110 (2013) 61–69. http://dx.doi.org/10.1016/j.microc.2013.02.006.
[29] A.E. Dolphin, A.H. Goodman, D.D. Amarasiriwardena, Variation in elemental intensities among teeth and between pre- and postnatal regions of enamel, Am. J. Phys. Anthropol. 128 (2005) 878–888. http://dx.doi.org/10.1002/ajpa.20213.
[30] A. Hanć, I. Komorowicz, M. Iskra, W. Majewski, D. Barałkiewicz, Application of spectroscopic techniques: icp-oes, LA-ICP-MS and chemometric methods for studying the relationships between trace elements in clinical samples from patients with atherosclerosis obliterans, Anal. Bioanal. Chem. 399 (2011) 3221–3231. http://dx.doi.org/10.1007/s00216-011-4729-5.
[31] T. Van Acker, S.J.M. Van Malderen, M. Van Heerden, J.E. McDuffie, F. Cuyckens, F. Vanhaecke, High-resolution laser ablation-inductively coupled plasma-mass spectrometry imaging of cisplatin-induced nephrotoxic side effects, Anal. Chim. Acta 945 (2016) 23–30. http://dx.doi.org/10.1016/j.aca.2016.10.014.
[32] M. Zoriy, A. Matusch, T. Spruss, J.S. Becker, Laser ablation inductively coupled plasma mass spectrometry for imaging of copper, zinc, and platinum in thin sections of a kidney from a mouse treated with cis-platin, Int. J. Mass Spectrom. 260 (2007) 102–106. http://dx.doi.org/10.1016/j.ijms.2006.09.012.
[33] E. Moreno-Gordaliza, C. Giesen, A. Lázaro, D. Esteban-Fernández, B. Humanes, B. Cañas, U. Panne, A. Tejedor, N. Jakubowski, M.M. Gómez-Gómez, Elemental bioimaging in kidney by LA-ICP-MS as a tool to study nephrotoxicity and renal protective strategies in cisplatin therapies, Anal. Chem. 83 (2011) 7933–7940. http://dx.doi.org/10.1021/ac201933x.
[34] N. Kamaly, J.A. Pugh, T.L. Kalber, J. Bunch, A.D. Miller, C.W. McLeod, J.D. Bell, Imaging of gadolinium spatial distribution in tumor tissue by laser ablation inductively coupled plasma mass spectrometry, Mol. Imaging Biol. 12 (2010) 361–366. http://dx.doi.org/10.1007/s11307-009-0282-4.
[35] I. Konz, B. Fernández, M.L. Fernández, R. Pereiro, H. González-Iglesias, M. Coca-Prados, A. Sanz-Medel, Quantitative bioimaging of trace elements in the human lens by LA-ICP-MS, Anal. Bioanal. Chem. 406 (2014) 2343–2348. http://dx.doi.org/10.1007/s00216-014-7617-y.
[36] A. Sussulini, E. Wiener, T. Marnitz, B. Wu, B. Müller, B. Hamm, J. Sabine Becker, Quantitative imaging of the tissue contrast agent $[Gd(DTPA)]^{2-}$ in articular cartilage by laser ablation inductively coupled plasma mass spectrometry, Contrast Media Mol. Imaging 8 (2013) 204–209. http://dx.doi.org/10.1002/cmmi.1509.
[37] C. Austin, D. Hare, A.L. Rozelle, W.H. Robinson, R. Grimm, P. Doble, Elemental bio-imaging of calcium phosphate crystal deposits in knee samples from arthritic patients, Metallomics 1 (2009) 142. http://dx.doi.org/10.1039/b901310p.
[38] D.S. Urgast, D.G. Ellingsen, B. Berlinger, E. Eilertsen, G. Friisk, V. Skaug, Y. Thomassen, J.H. Beattie, I.S. Kwun, J. Feldmann, Multi-elemental bio-imaging of rat tissue from a study investigating the bioavailability of bismuth from shotgun pellets, Anal. Bioanal. Chem. 404 (2012) 89–99. http://dx.doi.org/10.1007/s00216-012-6101-9.
[39] A.M. Ghazi, J.C. Wataha, N.L. O'Dell, B.B. Singh, R. Simmons, S. Shuttleworth, Quantitative concentration profiling of nickel in tissues around metal implants: a new biomedical application of laser ablation sector field ICP-MS, J. Anal. At. Spectrom. 17 (2002) 1295–1299. http://dx.doi.org/10.1039/b201678h.
[40] F. Blaske, O. Reifschneider, G. Gosheger, C.A. Wehe, M. Sperling, U. Karst, G. Hauschild, S. Höll, Elemental bioimaging of nanosilver-coated prostheses using X-ray fluorescence spectroscopy and laser ablation-inductively coupled plasma-mass spectrometry, Anal. Chem. 86 (2014) 615–620. http://dx.doi.org/10.1021/ac4028577.
[41] R.S. Flatebø, P.J. Høl, K.N. Leknes, J. Kosler, S.A. Lie, N.R. Gjerdet, Mapping of titanium particles in peri-implant oral mucosa by Laser Ablation Inductively Coupled Plasma Mass Spectrometry and high-resolution optical darkfield microscopy, J. Oral. Pathol. Med. 40 (2011) 412–420. http://dx.doi.org/10.1111/j.1600-0714.2010.00958.x.
[42] J. Draxler, A. Zitek, M. Meischel, S.E. Stranzl-Tschegg, B. Mingler, E. Martinelli, A.M. Weinberg, T. Prohaska, Regionalized quantitative LA-ICP-MS imaging of the biodegradation of magnesium alloys in bone tissue, J. Anal. At. Spectrom. 30 (2015) 2459–2468. http://dx.doi.org/10.1039/C5JA00354G.
[43] A. Sajnóg, A. Hanć, K. Makuch, R. Koczorowski, D. Barałkiewicz, Study on quantitative analysis of Ti, Al and V in clinical soft tissues after placing the dental implants by laser ablation inductively coupled plasma mass spectrometry, Spectrochim. Acta - Part B At. Spectrosc. 125 (2016) 1–10. http://dx.doi.org/10.1016/j.sab.2016.09.002.
[44] N. Miliszkiewicz, S. Walas, A. Tobiasz, Current approaches to calibration of LA-ICP-MS analysis, J. Anal. At. Spectrom. 30 (2015) 327–338. http://dx.doi.org/10.1039/C4JA00325J.
[45] D. Hare, C. Austin, P. Doble, Quantification strategies for elemental imaging of biological samples using laser ablation-inductively coupled plasma-mass spectrometry, Analyst 137 (2012) 1527. http://dx.doi.org/10.1039/c2an15792f.
[46] K. Jurowski, M. Szewczyk, W. Piekoszewski, M. Herman, B. Szewczyk, G. Nowak, S. Walas, N. Miliszkiewicz, A. Tobiasz, J. Dobrowolska-Iwanek, A standard sample preparation and calibration procedure for imaging zinc and magnesium in rats' brain tissue by laser ablation-inductively coupled plasma-time of flight-mass spectrometry, J. Anal. At. Spectrom. 29 (2014) 1425. http://dx.doi.org/10.1039/C3JA50378J.
[47] O. Reifschneider, C.A. Wehe, I. Raj, J. Ehmcke, G. Ciarimboli, M. Sperling, U. Karst, Quantitative bioimaging of platinum in polymer embedded mouse organs using laser ablation ICP-MS, Metallomics 5 (2013) 1440. http://dx.doi.org/10.1039/c3mt00147d.
[48] C. O' Connor, B.L. Sharp, P. Evans, On-line additions of aqueous standards for calibration of laser ablation inductively coupled plasma mass spectrometry: theory and comparison of wet and dry plasma conditions, J. Anal. At. Spectrom 21 (2006) 556. http://dx.doi.org/10.1039/b600916f.
[49] H.-J. Stärk, R. Wennrich, A new approach for calibration of laser ablation inductively coupled plasma mass spectrometry using thin layers of spiked agarose gels as references, Anal. Bioanal. Chem. 399 (2011) 2211–2217. http://dx.doi.org/10.1007/s00216-010-4413-1.
[50] A. Izmer, D. Gholap, K. De Houwer, F. Cuyckens, F. Vanhaecke, A pilot study on the use of laser ablation-ICP-mass spectrometry for assessing/mapping the distribution of a drug and its metabolites across the body compartments of rats, J. Anal. At. Spectrom. 27 (2012) 413. http://dx.doi.org/10.1039/c2ja10343e.
[51] C. Austin, D. Hare, T. Rawling, A.M. McDonagh, P. Doble, Quantification method for elemental bio-imaging by LA-ICP-MS using metal spiked PMMA films, J. Anal. At. Spectrom. 25 (2010) 722. http://dx.doi.org/10.1039/b911316a.
[52] M. Bonta, B. Hegedus, A. Limbeck, Application of dried-droplets deposited on pre-cut filter paper disks for quantitative LA-ICP-MS imaging of biologically relevant

minor and trace elements in tissue samples, Anal. Chim. Acta 908 (2016) 54–62. http://dx.doi.org/10.1016/j.aca.2015.12.048.
[53] M. Bonta, H. Lohninger, M. Marchetti-Deschmann, A. Limbeck, Application of gold thin-films for internal standardization in LA-ICP-MS imaging experiments, Analyst 139 (2014) 1521. http://dx.doi.org/10.1039/c3an01511d.
[54] M. Chudzinska, A. Debska, D. Baralkiewicz, Method validation for determination of 13 elements in honey samples by ICP-MS, Accredit. Qual. Assur. 17 (2012) 65–73. http://dx.doi.org/10.1007/s00769-011-0812-z.
[55] U. Meyer, M. Bühner, A. Büchter, B. Kruse-Lösler, T. Stamm, H.P. Wiesmann, Fast element mapping of titanium wear around implants of different surface structures, Clin. Oral. Implants Res. 17 (2006) 206–211. http://dx.doi.org/10.1111/j.1600-0501.2005.01184.x.
[56] B.W. Darvell, N. Samman, W.K. Luk, R.K.F. Clark, H. Tideman, Contamination of titanium castings by aluminium oxide blasting, J. Dent. 23 (1995) 319–322. http://dx.doi.org/10.1016/0300-5712(94)00003-X.
[57] N.M. Reed, R.O. Cairns, R.C. Hutton, Y. Takaku, Characterization of polyatomic ion interferences in inductively coupled plasma mass spectrometry using a high resolution mass spectrometer, J. Anal. At. Spectrom. 9 (1994) 881–896. http://dx.doi.org/10.1039/ja9940900881.
[58] H. Sela, Z. Karpas, M. Zoriy, C. Pickhardt, J.S. Becker, Biomonitoring of hair samples by laser ablation inductively coupled plasma mass spectrometry (LA-ICP-MS), Int. J. Mass Spectrom. 261 (2007) 199–207. http://dx.doi.org/10.1016/j.ijms.2006.09.018.
[59] A. Hanć, P. Zduniak, K. Erciyas-Yavuz, A. Sajnóg, D. Barałkiewicz, Laser ablation-ICP-MS in search of element pattern in feathers, Microchem. J. 134 (2017) 1–8. http://dx.doi.org/10.1016/j.microc.2017.04.043.
[60] A. Hanć, A. Piechalak, B. Tomaszewska, D. Barałkiewicz, Laser ablation inductively coupled plasma mass spectrometry in quantitative analysis and imaging of plant's thin sections, Int. J. Mass Spectrom. 363 (2014) 16–22. http://dx.doi.org/10.1016/j.ijms.2014.01.020.
[61] D.A. Frick, D. Günther, Fundamental studies on the ablation behaviour of carbon in LA-ICP-MS with respect to the suitability as internal standard, J. Anal. At. Spectrom. 27 (2012) 1294. http://dx.doi.org/10.1039/c2ja30072a.
[62] V. Zaichick, Chemical elements of human bone tissue investigated by nuclear analytical and related methods, Biol. Trace Elem. Res. 153 (2013) 84–99. http://dx.doi.org/10.1007/s12011-013-9661-4.
[63] C.M. Abraham, A brief historical perspective on dental implants, their surface coatings and treatments, Open Dent. J. 8 (2014) 50–55. http://dx.doi.org/10.2174/1874210601408010050.
[64] T. Rae, The biological response to titanium and titanium-aluminium-vanadium alloy particles, Biomaterials 7 (1986) 30–36. http://dx.doi.org/10.1016/0142-9612(86)90085-2.
[65] T. Rae, The biological response to titanium and titanium-aluminium-vanadium alloy particles, Biomaterials 7 (1986) 37–40. http://dx.doi.org/10.1016/0142-9612(86)90086-4.
[66] J. Babbush, C.A. Hahn, J.A. Krauser, J.T. Rosenlicht, Dental Implants: The Art and Science, 2nd ed., Saunders, 2010.
[67] X. Liu, P.K. Chu, C. Ding, Surface modification of titanium, titanium alloys, and related materials for biomedical applications, Mater. Sci. Eng. R. Rep. 47 (2004) 49–121. http://dx.doi.org/10.1016/j.mser.2004.11.001.
[68] S. Lee, B.T. Goh, S.H. Lai, H. Tideman, P.J.W. Stoelinga, J.A. Jansen, Peri-implant and systemic release of metallic elements following insertion of a mandibular modular endoprosthesis in Macaca fascicularis, Acta Biomater. 5 (2009) 3640–3646. http://dx.doi.org/10.1016/j.actbio.2009.05.028.
[69] A. Sicilia, S. Cuesta, G. Coma, I. Arregui, C. Guisasola, E. Ruiz, A. Maestro, Titanium allergy in dental implant patients: a clinical study on 1500 consecutive patients, Clin. Oral. Implants Res. 19 (2008) 823–835. http://dx.doi.org/10.1111/j.1600-0501.2008.01544.x.
[70] H. Matusiewicz, Potential release of in vivo trace metals from metallic medical implants in the human body: from ions to nanoparticles – a systematic analytical review, Acta Biomater. 10 (2014) 2379–2403. http://dx.doi.org/10.1016/j.actbio.2014.02.027.
[71] L. Balcaen, E. Bolea-Fernandez, M. Resano, F. Vanhaecke, Accurate determination of ultra-trace levels of Ti in blood serum using ICP-MS/MS, Anal. Chim. Acta 809 (2014) 1–8. http://dx.doi.org/10.1016/j.aca.2013.10.017.